Final Draft
of the original manuscript:

Dietzel, W.; Pfuff, M.; Juilfs, G.G.:

Hydrogen permeation in plastically deformed steel membranes

HYDROGEN PERMEATION IN PLASTICALLY DEFORMED STEEL MEMBRANES

W. DIETZEL[1], M. PFUFF[1], G. G. JUILFS[2]

[1] GKSS-Forschungszentrum Geesthacht GmbH, Max-Planck-Str. 1, D-21502
Geesthacht, Germany
[2] SAP AG, Neurottstraße 16, D-69190 Walldorf, Germany
wolfgang.dietzel@gkss.de

Abstract

In previously performed fracture mechanics SCC tests at pre-cracked C(T) specimens of a low alloy structural steel (FeE 690T) which had been in situ charged with hydrogen a correlation between the applied plastic deformation rate and the crack extension rate caused by hydrogen embrittlement had been established. To rationalise these results, the influence of the plastic strain on the hydrogen diffusion was studied in electrochemical permeation experiments. To this end, membrane specimens of the same steel were plastically deformed, either by cold rolling or by tensile straining, and the diffusion of atomic hydrogen in these membranes was measured in classical Devanathan-Stachursky experiments. From the hydrogen flux measured at the exit side in the form of current versus time curves effective diffusion coefficients were evaluated which exhibited a clear dependence on the strain. In addition, the diffusion was simulated by a model which assumes the trapping of the hydrogen atoms at sites which are generated by the plastic strain. For various values of the trap density, the evolution of the permeation current with time was calculated by numerically solving a non-linear diffusion equation. From these calculated permeation curves, effective diffusion coefficients were determined using the same time lag procedure which had been applied to the experimental data. The results thus obtained were found to be in good agreement with the experimentally obtained data.

Keywords: effective diffusion coefficient, hydrogen embrittlement, hydrogen permeation, plastic deformation.

1. Introduction

In previous work, pre-cracked C(T) specimens of the low alloy structural steel FeE 690T had been investigated in fracture mechanics SCC tests by subjecting these specimens to various constant load-line displacement rates, ranging from 1 µm/h to 30 mm/h, while the specimens were in situ charged with hydrogen [1]. In these earlier tests, the crack tip opening displacement, CTOD, had been employed to characterise the crack growth resistance of the material under investigation. The values of the CTOD were in each test directly measured in the form of the so-called δ_5 parameter by using specifically designed clip gauges which were attached to the specimens side faces in the vicinity of the fatigue pre-crack tip [1-3]. Crack growth rates, da/dt, were determined from measurements of the actual crack lengths performed by using the DC potential drop technique.

The crack growth rates, da/dt, measured in these displacement controlled tests become essentially constant once the initiation stage is passed [1]. By plotting the plateau or steady state values, $da/dt_{plateau}$, of these rates as a function of the applied deformation rates measured as the change of the parameter δ_5 with time, $d\delta_5/dt$, a correlation between the rate of change in plastic deformation on the one side and the crack extension rate due to hydrogen embrittlement on the other side could be established. A typical feature of this correlation is, that at low deformation rates, in this case below 10^{-5} mm/s, the curve for the corrosive

environment deviates from the straight line relationship which in a log-log presentation of the data is characteristic of tests in air (Fig. 1). This finding indicated that the displacement rate, and hence the rate at which the plastic deformation is imposed on the specimen, plays a dominating role in the phenomenon of hydrogen embrittlement of this material.
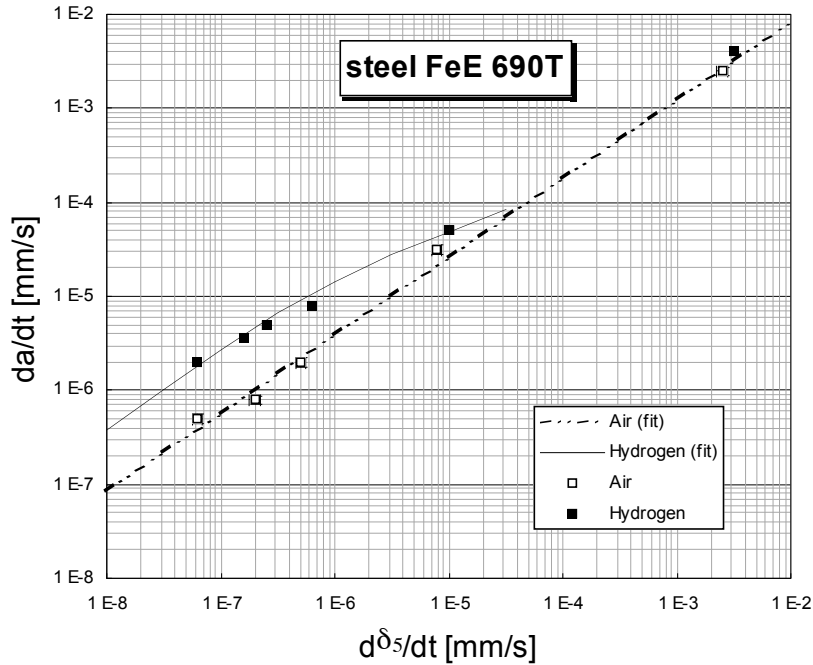

Fig. 1: Relationship between the applied deformation rate, $d\delta_5/dt$, and the crack growth rate, da/dt, measured in rising displacement tests at pre-cracked C(T) specimens in air (dashed line) and under hydrogen charging (solid line) [1].

To rationalise these observations, the influence of the plastic strain on the hydrogen diffusion in steel was studied in electrochemical permeation experiments in which the hydrogen permeation was measured in steel membranes which were deformed to various degrees of plastic strain.

2. Experimental Details and Data Evaluation

The permeation tests were performed on the same fine grained low alloy structural steel with the European designation FeE 690T which had been used to obtain the results shown in Fig. 1. The quenched and tempered material (trade name "N-A-XTRA 70", Thyssen Stahl AG) had the chemical composition given in Table 1 and mechanical properties according to Table 2. Typical pictures of the microstructure of this steel are shown in Fig 2.

Table 1: Chemical composition of the steel FeE 690T (% by weight).

C	Si	Mn	P	S	Cr	Mo	Zr
0.18	0.67	1.02	0.009	0.003	0.85	0.48	< 0.12

Table 2: Mechanical properties of the steel FeE 690T (room temperature).

Material	$R_{p0.2}$ [MPa]	R_m [MPa]	A [%]
steel FeE 690T	695	820	15

25 µm

5 µm
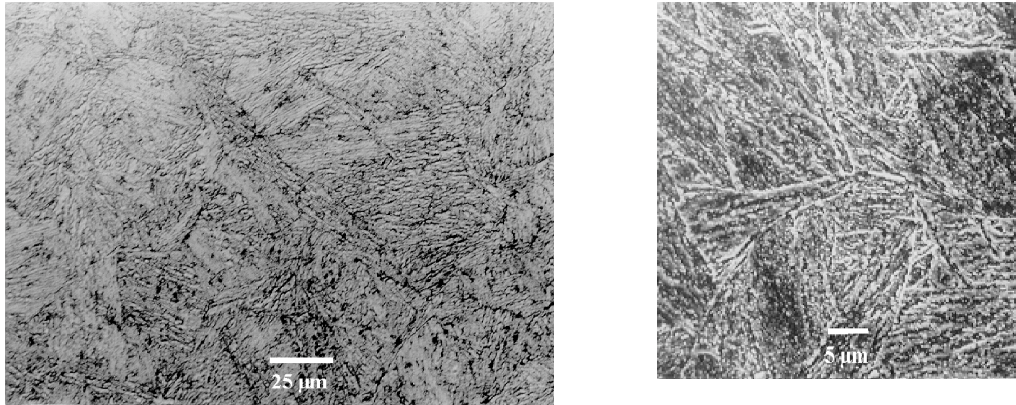
Fig. 2: Microstructure of the steel FeE 690T in lower (left) and higher (right) magnification (2% Nital etch).

a

3 mm

RD
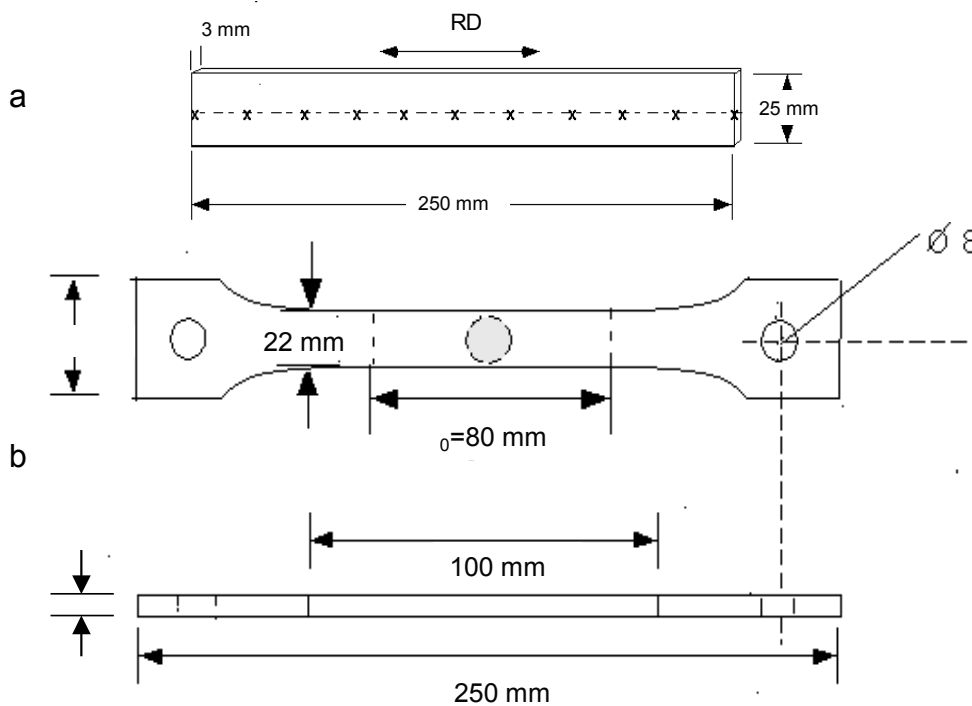
25 mm

250 mm

Ø 8

22 mm

$_0$=80 mm

b

100 mm

250 mm

Fig. 3: Specimens for permeation experiments on strained membranes,
a: cold rolled bars with plastic strain between 10 and 60 %,
b: flat tensile specimens with plastic strain between 0 and 6.5 %

From this material, thin foils were prepared and were subjected to plastic deformation. This was either done prior to testing by cold rolling the material or, during the tests, via in situ straining of flat tensile specimens (Figs. 3a and b). The hydrogen permeation through

these specimens was studied by electrochemical permeation experiments in a 0.1M NaOH solution at 298 K using the classical Devanathan-Stachursky technique illustrated in Fig. 4 [4]. Details of this experimental work are given elsewhere [5].
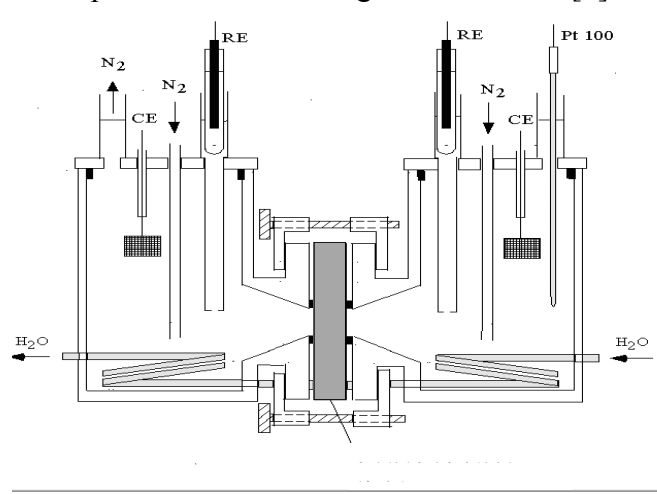

Fig. 4:   Experimental set-up for measuring the diffusion coefficient, D (CE: counter electrode, RE: reference electrode, WE: working electrode)

3. Experimental Results

In Fig. 5, a set of permeation curves is shown, in which the normalized current density, i_p/i_p^{max}, which have been measured at the exit side of the differently strained specimens is plotted with time. As can be seen, the time that it takes before the first increase in the current signal on the detection side is measured, i.e., the breakthrough time or time lag, t_b, depends on the amount of plastic strain which the specimen under investigation has seen. However, it should be pointed out that the maximum hydrogen flux and hence the maximum permeation current density, i_p^{max}, measured in the plateau region of each of the permeation curves remained practically unchanged in all tests.

From the curves of the permeation current shown in Fig. 5, effective diffusion coefficients, D_{eff}, were determined using the well known time lag method and making use of the fact that the time lag is inversely proportional to the effective diffusion coefficient by:

$$t_b = 0.5 \frac{L^2}{\pi^2 D_{eff}} \tag{1}$$

where t_b is the time lag and L is the membrane thickness. These effective diffusion coefficients are in Fig. 6 plotted as a function of the degree of plastic deformation, ε_{pl}, which was imposed on the specimen prior to or during each test.
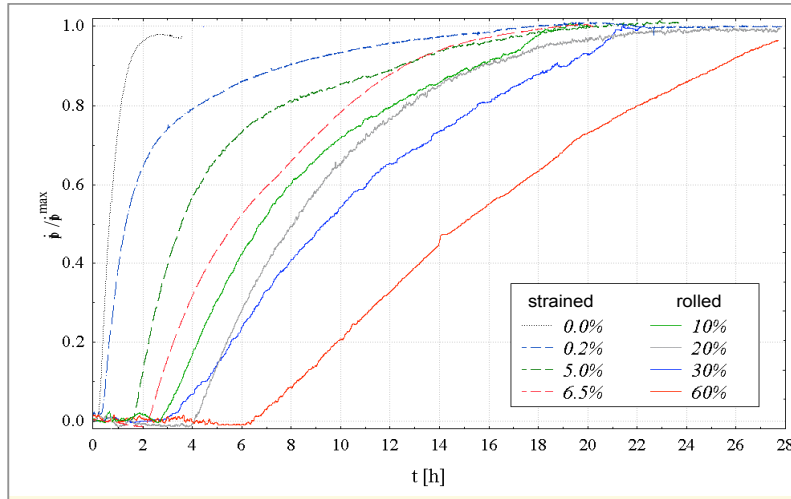
Fig. 5: Permeation curves showing the normalized current density, $i_p/i_p{}^{max}$, for different degrees of plastic deformation, ε_{pl}, measured at the steel FeE 690T in 0.1M NaOH, (Ec = -1.3 V, T = 293 K).

As can be seen, in the log-log plot used in Fig. 6 the effective diffusion coefficients which were thus determined from the permeation curves show a clear linear dependence on the degree of plastic strain, ε_{pl}, above a strain value of 0.5%.
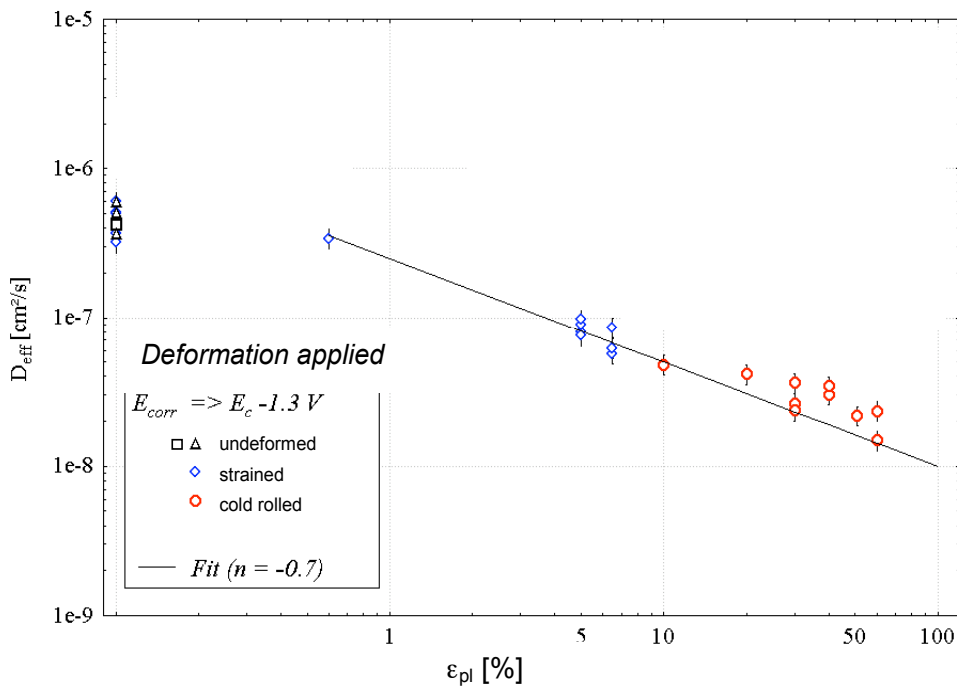

Fig. 6: Effective diffusion coefficient as a function of plastic strain (charging at a potential of -1.3 V vs. Ag/AgCl electrode).

4. Model Calculations

The permeation dependence according to Fig. 6 was simulated using a transport model that is based on work of Oriani [6] and of Johnson and Lin [7]. The model has been applied by Krom et al.[8] to simulate the hydrogen distribution near a blunting crack. In this model, it is assumed that a fraction of the hydrogen atoms that diffuse through lattice sites are trapped in trap sites which are generated by the plastic deformation imposed on the material. Assuming that the trap density is not depending on time and that the gradient of the hydrostatic stress vanishes, the differential equation can be modified to

$$\frac{C_L + C_T(1 - \theta_T)}{C_L}\frac{\partial C_L}{\partial t} - D_L \Delta C_L = 0 . \tag{2}$$

Here, C_L and C_T are the density of hydrogen in lattice sites and in traps, respectively. θ_T is the occupancy of traps, i.e. $\theta_T = C_T / N_T$ where N_T is the density of trap sites in the material. D_L is the diffusion coefficient of hydrogen in a trap free material. Assuming thermodynamic equilibrium, the density of the trapped hydrogen can be related to the density of lattice hydrogen through [6]

$$C_T = \frac{N_T}{1 + \dfrac{N_L}{K_T C_L}} , \tag{3}$$

K_T, the Boltzmann factor which quantifies the ratio between trap and lattice occupancy is related to the binding energy of hydrogen in traps relative to the lattice, ΔE_T, by [6]

$$K_T = e^{-\Delta E_T / RT} \tag{4}$$

(R : universal Gas constant, T: absolute temperature in K).

For thin membranes, equation (2) can be limited to the spatial co-ordinate perpendicular to the membrane surface. This equation was numerically solved using a finite difference scheme according to W. H. PRESS et al [9], and by keeping the values of the hydrogen concentration on both faces of the membrane fixed. Under the assumption that every hydrogen atom that reaches the anodic side of the membrane is oxidised, the hydrogen density becomes equal to zero at this surface. At the entry side, the hydrogen concentration is determined by the electro-chemical conditions at the boundary between electrolyte and solid. Using Faraday's constant, this value can be calculated from the permeation as $C_{L0} = 2.1 \; 10^{23}/m^3$.

Thus, from this simulation the anodic current was obtained as a function of time for different values of the trap density. In the same manner as in the case of the experimentally obtained time dependent permeation current curves, the time lag and hence the effective diffusion coefficients were determined from the calculated data.

The model calculations reveal that the effective diffusion coefficients thus determined from the calculated permeation current curves are inversely proportional to the trap density for high values of this density. On the other hand, in the double logarithmic presentation of the experimentally determined effective diffusion coefficient versus the plastic deformation shown in Fig. 6, a linear behaviour with a slope of approximately -0.7 can be identified at deformations higher than 0.5%. The same dependence will therefore result from the simulations as the asymptotic behaviour for large deformations if the trap density, N_T, is assumed to be related to the plastic deformation, ε_{pl}, by

$$N_T = N_{T0} + N_{T1}\,\varepsilon_{pl}^{0.7} \tag{5}$$

with the constants N_{T0} and N_{T1} to be determined by comparing the measured effective diffusion coefficients and the calculated ones.
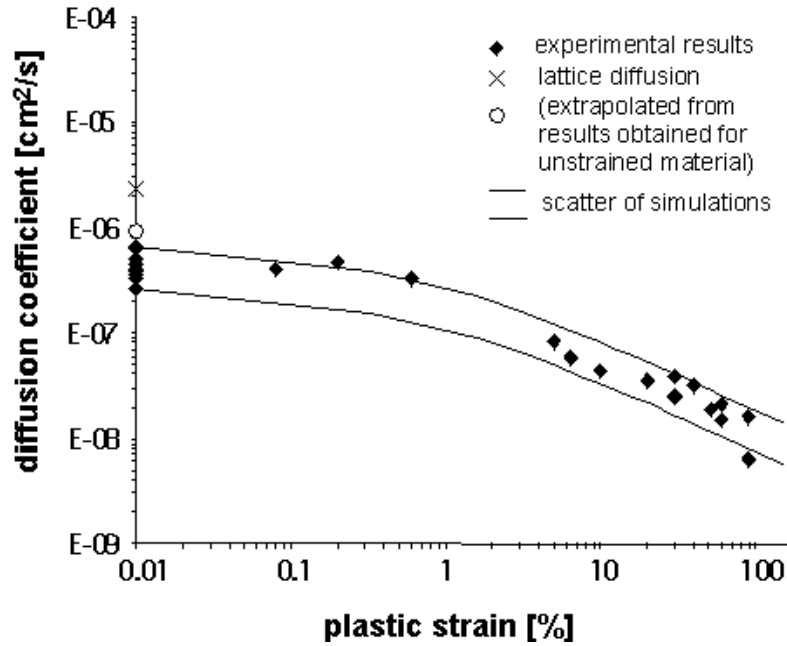

Fig. 7: Comparison of experimentally determined effective diffusion coefficients (points, c.f. Fig. 6) and results of simulations (lines) .

As can be seen from Fig. 7, the measured effective diffusion coefficients as a function of the plastic strain fall into the scatter band of the simulation results which were obtained by setting $N_{T0} = 8.8 \ 10^{22}/m^3$ and $N_{T1} = 4.8 \ 10^{24}/m^3$. The scatter of the simulations results from the scatter of the diffusion coefficient for unstrained material. This latter had been measured on different specimens of the same material and geometry and appears on the Y-axis of the diagrams in Figs. 6 and 7.

Following Eq. (5) the trap density does not vanish for unstrained material and is equal to $8.8 \ 10^{22}/m^3$. This relatively small density of traps may be due to dislocations which are still present in the unstrained material or to grain and/or phase boundaries. When assuming zero trap density the calculation yields an upper and lower value of the diffusion coefficient which both correspond to D values of a virtually trap free material and is thus representative of pure lattice diffusion as is indicated in Fig. 7.

5. Discussion

According to Eq. (3), the occupancy of traps, θ_T, with hydrogen depends on the Boltzmann factor K_T. The simulated dependence of the effective diffusion coefficient on the plastic strain shown in Fig. 7 was obtained by setting $K_T = 2.91 \ 10^7$. From this value, the binding energy of hydrogen in traps can be derived to be 42.1 kJ/mol. This value is lower than the value given above for edge dislocation cores, and reflects the fact that hydrogen is in reality bonded to different kinds of traps with different binding energies, like edge or screw dislocations and grain or phase boundaries.

6. Conclusions

Permeation experiments on plastically deformed foils prepared from the ferritic steel FeE 690T showed that the effective diffusion coefficient depends on the plastic strain and on the overall hydrogen concentration, whereas the maximum hydrogen flux remained almost unchanged. These observations are in agreement with work of HUTCHINGS and TURNBULL [10] and of KURKELA et al. [11] for other types of steel, and can be rationalised in terms of variations of the dislocation density acting as 'sinks' for the diffusible hydrogen atoms. When comparing the experimental data with the results of model calculations that treat the hydrogen transport in an idealised way as a diffusion process in the presence of only one kind of deep traps, a good agreement was observed for the entire range of plastic strain that was investigated. Together with the results of previous studies concerning the influence of hydrogen on the fracture toughness, the permeation data obtained in this work suggest that the observed influence of deformation rates on the fracture mechanism can be attributed to the reduced mobility of hydrogen atoms in the plastic zone.

7. References

[1]   *M. Pfuff, W. Dietzel* Rising Displacement Testing of Hydrogen Embrittlement, in: Problems of Corrosion and Corrosion Protection of Materials, Lviv, 2002, Physico-Chemical Mechanics of Materials, Special Issue No 3, pp. 268-273

[2]   *D. Hellmann, K.-H. Schwalbe* On the Experimental Determination of CTOD Based R-Curves, in: The Crack Tip Opening Displacement in Elastic-Plastic Fracture Mechanics, K.-H. Schwalbe ed., Springer Verlag, Berlin-Heidelberg-New York, 1986, pp. 115-132.

[3]   *W. Dietzel* The Use of Crack Tip Opening Displacement for Testing of Hydrogen Embrittlement of High Strength Steels, Fiziko-Chimiceskaja Mechanika Materialov / Physico-Chemical Mechanics of Materials, Vol 6 (2004), pp. 35-40..

[4]   *M. A. V. Devanathan, Z. Stachursky* The absorption and diffusion of electrolytic Hydrogen in palladium, Proc. Roy. Soc., **A 270**, 1962, 90-102.

[5]   *G. G. Juilfs* Das Diffusionsverhalten von Wasserstoff in einem niedriglegierten Stahl unter Berücksichtigung des Verformungsgrades und der Deckschichtbildung in alkalischen Medien (Ph.D. Thesis), Report GKSS 2001/16, GKSS, 2001.

[6]   *R. A. Oriani* The diffusion and trapping of hydrogen in steel, Acta Metall. 18, 1970, 147-157.

[7]   *H. H. Johnson and R. W. Lin* Hydrogen deuterium trapping in iron, Hydrogen Effects in Metal, I. M. Bernstein and A. W. Thompson eds., Metallurgical Society of AIME, New York, 1981, 3-23.

[8]   *A. H. M. Krom, R. W. J. Koers, and A. Bakker* Hydrogen transport near a blunting crack, J. Mech. Phys. Solids, 47, 1999, 971-992.

[9]   *W. H. Press, B. P. Flannery, S. A. Teukolsky, and W. T. Vetterling* Numerical Recipes, The Art of Scientific Computing, Cambridge University Press, Cambridge, 1986.

[10] *R. B. Hutchings and A. Turnbull* The effect of prior mechanical deformation on Hydrogen transport through 13 % chromium martensitic stainless steel, Corrosion Science, 33, 5, 1992, 713-728.

[11] *M. Kurkela, G. S. Frankel, R. M. Latanision, S. Suresh, and R. O. Ritchie* Influence of Plastic Deformation on Hydrogen Transport in 2 1/4 Cr-1Mo steel, Scripta Met., 16, 1982, 455-459.